Inorg. Chem. **2006**, *45*, 10363–10370

Supramolecular Structures and Columnar Mesophase Induction in Nondiscoid Pyrazoles by Complexation to Rhodium(I)

Raquel Giménez,*,† Anabel Elduque,*,‡ José Antonio López,‡ Joaquín Barberá,† Emma Cavero,† Ignacio Lantero,‡ Luis A. Oro,‡ and José Luis Serrano†

Departamento de Química Orgánica and Departamento de Química Inorgánica, Facultad de Ciencias—Instituto de Ciencia de Materiales de Aragón, Universidad de Zaragoza-CSIC, 50009 Zaragoza, Spain

Received July 28, 2006

Several new *cis*-[RhCl(CO)$_2$(Ln)] complexes have been prepared using different polycatenar pyrazole ligands (Ln) in order to obtain columnar liquid crystalline arrangements. The topology of the ligand plays an essential role, and a mesophase is induced at room temperature from a nonmesogenic pyrazole only when it is symmetrically substituted with six decyloxy chains. The single-crystal structure of a methoxy-substituted analogue, 3,5-bis(3,4,5-trimethoxyphenyl)pyrazole, is formed by globular tetrameric structures held together by H-bonding. However, parallel dimers are present in the corresponding *cis*-chlorodicarbonylrhodium(I) complex, a situation that explains the induction of a columnar mesophase in the decyloxy-substituted complex. The XRD pattern of the mesophase is consistent with a hexagonal symmetry in which the columns are formed by molecules assembled in an antiparallel mode. The crystal-to-mesophase transition was also detected by spectroscopic techniques as a shift in the IR carbonyl stretching bands and the appearance of a charge-transfer band in the absorption spectrum with thermochromic behavior.

Introduction

Square-planar d^8 rhodium(I) or iridium(I) complexes are interesting for molecular electronics as their disposition along a columnar axis may give rise to extended metallic interactions[1] and result in materials with anisotropic semiconductive[2−4] or pyroelectric[5,6] properties. Materials with metal arrangements having different bond strengths, usually weaker than a covalent intermetallic bond, have been prepared by growing good quality single crystals or by LB film deposition. A third strategy that could lead to analogous arrangements, and related to this work, is the generation of columnar liquid crystal phases from these types of metal complexes[7] (named metallomesogens). This approach is a way to combine the self-organizational ability of the mesogens and the different properties introduced by the metal center.

There are several drawbacks associated with metallomesogens,[8−10] and one is that the geometry imposed by the metal is not always compatible with a columnar organization of molecules. A second drawback is the difficulty in preserving the liquid crystalline order at room temperature as metal complexes usually have high melting points. For these reasons, careful design of the ligand is needed in order to overcome these situations.[11,12] Although the most favorable shape for columnar liquid crystals is the discoid shape, in

* To whom correspondence should be addressed. E-mail: rgimenez@unizar.es (R.G.), anaelduq@unizar.es (A.E.).
† Departamento de Química Orgánica.
‡ Departamento de Química Inorgánica.

(1) Bera, J. K.; Dunbar, K. R. *Angew. Chem., Int. Ed.* **2002**, *41*, 4453−4457.
(2) Pitt, C. G.; Monteith, L. K.; Ballard, L. F.; Collman, J. P.; Morrow, J. C.; Roper, W. R.; Ulkii, D. *J. Am. Chem. Soc.* **1966**, *88*, 4286−4287.
(3) Aullón, G.; Alvarez, S. *Chem.—Eur. J.* **1997**, *3*, 655−664.
(4) Miller, J. S.; Epstein, A. J. In *Progress in Inorganic Chemistry*; Lippard, S. J., Ed.; John Wiley and Sons: New York, 1976; Vol. 20.
(5) Richardson, T.; Topaçli, a.; Majid, W. H. A.; Greenwood, M. B.; Bruce, D. W.; Thornton, A.; Marsden, J. R. *Adv. Mater. Opt. Electron.* **1994**, *4*, 243−251.
(6) Wong, J. E.; Bruce, D. W.; Richardson, T. H. *Synth. Met.* **2005**, *148*, 11−14.
(7) Trzaska, S. T.; Swager, T. M. *Chem. Mater.* **1998**, *10*, 438−443.
(8) Serrano, J. L. *Metallomesogens: Synthesis, Properties and Applications*; VCH: Weinheim, 1996.
(9) Giménez, R.; Lydon, D. P.; Serrano, J. L. *Curr. Opin. Solid State Mater. Sci.* **2002**, *6*, 527−535.
(10) Donnio, B.; Guillon, D.; Deschenaux, R.; Bruce, D. W. In *Comprehensive Coordination Chemistry II*; McCleverty, J. A., Meyer, J. J., Eds.; Elsevier: Oxford, 2003; Vol. 7, p 357−627.
(11) Giménez, R.; Manrique, A. B.; Uriel, S.; Barberá, J.; Serrano, J. L. *Chem. Commun.* **2004**, 2064−2065.
(12) Terazzi, E.; Suarez, S.; Torelli, S.; Nozary, H.; Imbert, D.; Mamula, O.; Rivera, J.-P.; Guillet, E.; Benech, J.-M.; Bernardinelli, G.; Scopelliti, R.; Donnio, B.; Guillon, D.; Bünzli, J.-C. G.; Piguet, C. *Adv. Funct. Mater.* **2006**, *16*, 157−168.

10.1021/ic0614216 CCC: $33.50
Published on Web 11/15/2006

some cases a subtle combination of noncovalent dipole−dipole,[7,13−16] ligand−ligand and/or ligand−metal[17−23] or weak metal−metal[7,13,15] interactions can induce or stabilize a columnar mesophase with nondiscoid molecules. These interactions promote time-averaged disklike structures that self-organize to form columns. The only report of columnar mesomorphism in rhodium and iridium compounds described in the literature is an example of this behavior and concerns dicarbonyl-1,3-diketonate complexes $[M(CO)_2(dk)]$.[7]

In previous publications, we have reported that pyrazoles are versatile heterocycles for the generation of coordination compounds with columnar phases at or near room temperature.[24−27] Modulation of the intermolecular forces can be achieved in several ways using pyrazoles, either by incorporating appropriate substituents on the carbon atoms, through hydrogen bonding (as the pyrazole is a good donor and acceptor of such bonds) and/or by coordination to metals. Mononuclear rhodium complexes of the type *cis*-$[RhCl(CO)_2$-(HPz)] could be good candidates to show liquid crystallinity due to the properties observed for the related 1,3-diketonate complexes $[Rh(CO)_2(dk)]$. The presence of both the chloro ligand and the NH-pyrazole introduces additional dipolar and hydrogen bond interactions that may give rise to different molecular packing from diketonates and have a decisive influence on the properties.

Complexes with a similar structure {*cis*-$[MCl(CO)_2(L)]$, where M = Rh, Ir and L = nitrile,[28] pyridine,[29,30] or stilbazole[31,32]} have been studied in the field of liquid crystals, but columnar mesomorphism has never been found. In the case where L = pyrazole, it was observed that the mesomorphic properties of the ligand are worse[33] and only one compound (with nematic mesomorphism) has been reported.[34]

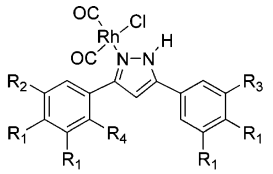

Compound **1**: $[RhCl(CO)_2(\mathbf{L1})]$, $R_1 = OC_{10}H_{21}$; R_2, R_3, R_4 = H
Compound **2**: $[RhCl(CO)_2(\mathbf{L2})]$, R_1, $R_2 = OC_{10}H_{21}$; R_3, R_4 = H
Compound **3**: $[RhCl(CO)_2(\mathbf{L3})]$, R_1, $R_2 = OC_{14}H_{29}$; R_3, R_4 = H
Compound **4**: $[RhCl(CO)_2(\mathbf{L4})]$, R_1, R_3, $R_4 = OC_{10}H_{21}$; R_2 = H
Compound **5**: $[RhCl(CO)_2(\mathbf{L5})]$, R_1, R_2, $R_3 = OC_{10}H_{21}$; R_4 = H
Compound **6**: $[RhCl(CO)_2(\mathbf{L6})]$, R_1, R_2, $R_3 = OCH_3$; R_4 = H

Figure 1. Structures of the rhodium complexes **1**−**6**.

In the work described here, several *cis*-$[RhCl(CO)_2(Hpz)]$ compounds (**1**−**6**, Figure 1) containing HPz ligands derived from different 3,5-diarylpyrazoles (**L1**−**L6**) were prepared. To promote columnar mesomorphism, the pyrazole ligands are substituted at the phenyl rings with four, five, or six long alkoxy chains (complexes **1**−**5**). These different substitution patterns allowed us to assess the influence of the structure of the pyrazole ligand on the formation of columnar phases. Finally, model compound **6** and its respective pyrazole **L6** were structurally characterized in the solid state in order to gain an insight into the tendency of these compounds to form columnar assemblies.

Experimental Section

Materials. The preparation of the metal complexes was carried out at room temperature under argon using standard Schlenk techniques. Pyrazole ligands **L1**−**L6**[27] and $[Rh(\mu\text{-}Cl)(CO)_2]_2$[35] were prepared according to literature methods. Dichloromethane was dried over calcium hydride and distilled under argon prior to use. Deuterated chloroform for NMR experiments was stirred with sodium carbonate and filtered prior to use.

Instrumentation. Elemental analysis was performed with a Perkin-Elmer 240C microanalyzer. IR spectra were measured on a Nicolet Avatar FTIR instrument using KBr pellets. ^{1}H NMR spectra were recorded on Bruker ARX 300 or Avance 400 spectrometers. Mass spectra were obtained with a VG Autospec spectrometer with positive ion FAB-LSIMS using nitrobenzyl alcohol as matrix. Optical absorption spectra were recorded with a UV4-200 UV−vis spectrophotometer from ATI-Unicam. Mesomorphic behavior and transition temperatures were determined using an Olympus BH-2 polarizing microscope equipped with a Linkam THMS 600 hot-stage central processor and a CS196 cooling system. Differential scanning calorimetry (DSC) was carried out using a DSC 2910 from TA Instruments with samples sealed in aluminum pans and a scanning rate of 10 °C/min under a nitrogen atmosphere. The apparatus was calibrated with indium (156.6 °C, 28.4 J g^{-1}) as the

(13) Coco, S.; Díez-Expósito, F.; Espinet, P.; Fernández-Mayordomo, C.; Martín-Álvarez, J. M.; Levelut, A. M. *Chem. Mater.* **1996**, *8*, 3666−3671.
(14) Morale, F.; Date, R. W.; Guillon, D.; Bruce, D. W.; Finn, R. L.; Wilson, C.; Blake, A. J.; Schröder, M.; Donnio, B. *Chem.—Eur. J.* **2003**, *9*, 2484−2501.
(15) Coco, S.; Espinet, P.; Martín-Álvarez, J. M.; Levelut, A. M. *J. Mater. Chem.* **1997**, *7*, 19−23.
(16) Barberio, G.; Bellusci, A.; Crispini, A.; Ghedini, M.; Golemme, A.; Prus, P.; Pucci, D. *Eur. J. Inorg. Chem.* **2005**, 181−188.
(17) Serrette, A. G.; Swager, T. M. *J. Am. Chem. Soc.* **1993**, *115*, 8879−8880.
(18) Zheng, H.; Lai, C. K.; Swager, T. M. *Chem. Mater.* **1994**, *6*, 101−103.
(19) Atencio, R.; Barberá, J.; Cativiela, C.; Lahoz, F. J.; Serrano, J. L.; Zurbano, M. M. *J. Am. Chem. Soc.* **1994**, *116*, 11558−11559.
(20) Serrette, A. G.; Swager, T. M. *Angew. Chem., Int. Ed. Engl.* **1994**, *33*, 2342−2345.
(21) Cocker, T. M.; Bachman, R. E. *Mol. Cryst. Liq. Cryst.* **2004**, *408*, 1−19.
(22) Lai, C. K.; Pang, Y. S.; Tsai, C. H. *J. Mater. Chem.* **1998**, *8*, 2605−2610.
(23) Terazzi, E.; Benech, J. M.; Rivera, J. P.; Bernardinelli, G.; Donnio, B.; Guillon, D.; Piguet, C. *Dalton Trans.* **2003**, 769−772.
(24) Barberá, J.; Giménez, R.; Serrano, J. L. *Adv. Mater.* **1994**, *6*, 470−472.
(25) Barberá, J.; Elduque, A.; Giménez, R.; Oro, L. A.; Serrano, J. L. *Angew. Chem., Int. Ed. Engl.* **1996**, *35*, 2832−2835.
(26) Barbera, J.; Elduque, A.; Gimenez, R.; Lahoz, F. J.; Lopez, J. A.; Oro, L. A.; Serrano, J. L. *Inorg. Chem.* **1998**, *37*, 2960−2967.
(27) Barberá, J.; Giménez, R.; Serrano, J. L. *Chem. Mater.* **2000**, *12*, 481−489.
(28) Bruce, D. W.; Lalinde, E.; Styring, P.; Dunmur, D. A.; Maitlis, P. M. *J. Chem. Soc., Chem. Commun.* **1986**, 581−582.
(29) Esteruelas, M. A.; Sola, E.; Oro, L. A.; Ros, M. B.; Serrano, J. L. *Chem. Commun.* **1989**, 55−56.
(30) Esteruelas, M. A.; Sola, E.; Oro, L. A.; Ros, M. B.; Marcos, M.; Serrano, J. L. *J. Organomet. Chem.* **1990**, *387*, 103−111.
(31) Bruce, D. W.; Dunmur, D. A.; Esteruelas, M. A.; Hunt, S. E.; Lelagadec, R.; Maitlis, P. M.; Marsden, J. R.; Sola, E.; Stacey, J. M. *J. Mater. Chem.* **1991**, *1*, 251−254.
(32) Adams, H.; Bailey, N. A.; Bruce, D. W.; Hudson, S. A.; Marsden, J. R. *Liq. Cryst.* **1994**, *16*, 643−653.
(33) Torralba, M. C.; Cano, M.; Campo, J. A.; Heras, J. V.; Pinilla, E.; Torres, M. R. *J. Organomet. Chem.* **2002**, *654*, 150−161.
(34) Barbera, J.; Elduque, A.; Gimenez, R.; Lahoz, F. J.; Lopez, J. A.; Oro, L. A.; Serrano, J. L.; Villacampa, B.; Villalba, J. *Inorg. Chem.* **1999**, *38*, 3085−3092.
(35) Hieber, W.; Lagally, H. *Z. Anorg. Allg. Chem.* **1943**, *251*, 96.

standard. Powder X-ray diffraction experiments were carried out using a Pinhole camera (Anton Paar) operating with a Ni-filtered Cu Kα beam. The sample was held in a Lindemann glass capillary (1 mm diameter) and heated with a variable-temperature attachment. The X-ray patterns were collected on flat photographic films.

General Procedure for the Synthesis of the Mononuclear Rhodium Complexes *cis*-[RhCl(CO)$_2$(Ln)], 1−6. To a solution of [Rh(μ-Cl)(CO)$_2$]$_2$ (15.6 mg, 0.04 mmol) in dry dichloromethane (10 mL) was added a solution of the appropriate pyrazole ligand (0.08 mmol in 15 mL of dry dichloromethane). The reaction mixture was stirred for 30 min, and the volume reduced to 0.5 mL. The addition of methanol led to the precipitation of a yellow solid or a yellow oil. The solids were purified by recrystallization from methanol, and the oils were washed several times with methanol and dried under vacuum. Oily samples crystallized as yellow solids upon storage in the refrigerator for several days. Yields: 80−90%.

Compound 1. Found: C, 65.9; H, 8.9; N: 2.7. Calcd for $C_{57}H_{92}ClN_2O_6Rh$: C, 65.8; H, 8.9; N, 2.7%. ν_{max}(KBr)/cm^{-1} 3198, 3179, 3150, 3129 (N−H), 2083, 2069, 2016, 2005 (CO), 1608, 1516 (arC−C), 1266, 1244 (C−O). δ_H (300 MHz; $CDCl_3$; Me_4Si) 0.84−0.88 (m, 12H, CH_3−), 1.25−1.50 (m, 56H, −CH_2−), 1.80−1.84 (m, 8H, −*CH_2*−CH_2−O−), 4.01−4.07 (m, 8H, −CH_2−O−), 6.56 (s, 1H, He), 6.91 (d, J = 8.5 Hz, 1H, Hh), 6.99 (d, J = 8.5 Hz, 1H, Hb), 7.09 (d, J = 2.0 Hz, 1H, Hg), 7.11 (dd, J = 8.5 Hz, J = 2.0 Hz, 1H, Hd), 7.24 (m, 2H, Ha, Hc), 11.63 (s, 1H, Hf). δ_C (75 MHz; $CDCl_3$; Me_4Si) 14.1 (CH_3−), 22.6, 26.0, 29.1, 29.2, 29.3, 29.4, 29.5, 31.9 (−CH_2−), 69.2, 69.5 (−CH_2−O−), 102.8 (═CH− pyrazole), 111.3, 113.2, 113.5, 114.9, 118.9, 119.8 (Car-H), 122.4, 124.5 (Car-pz), 145.5, 149.0, 149.6, 150.8, 157.1 (Car-O, Cpz). m/z (FAB$^+$) 1004 [M − Cl]$^+$.

Compound 2. Found: C, 67.3; H, 9.4; N, 2.3. Calcd for $C_{67}H_{112}ClN_2O_7Rh$: C, 67.3; H, 9.4; N, 2.3%. ν_{max}(KBr)/cm^{-1} 3197, 3172, 3128 (N−H), 2087, 2074, 2003 (CO), 1591, 1506 (arC−C), 1262 (C−O). δ_H (300 MHz; $CDCl_3$; Me_4Si) (see also Figure 2) 0.88 (m, 15H, CH_3−), 1.27−1.45 (m, 60H, −CH_2−), 1.45−1.55 (m, 10H, −CH_2−), 1.73−1.84 (m, 10H, −*CH_2*−CH_2−O−), 3.98−4.09 (m, 10H, −CH_2−O−), 6.59 (s, 1H, He), 6.71 (s, 0.8H, Hd), 6.9 (s, 1.2H, Hd′), 6.94 (d, J = 8.4 Hz, 0.6H, Hb′), 6.97 (d, J = 8.4 Hz, 0.4H, Hb), 7.03 (d, J = 2.0 Hz, 0.6H, Hc′), 7.13 (dd, J = 8.4 Hz, J = 2 Hz, 0.6H, Ha′), 7.26 (m, 0.8H, Ha, Hc), 11.62 (s, 0.4H, Hf), 11.70 (s, 0.6H, Hf′). δ_C (75 MHz; $CDCl_3$; Me_4Si, partial) 14.1 (CH_3−), 22.7, 25.9, 26.1, 28.8, 28.9, 29.0, 29.1, 29.2, 29.3, 29.4, 29.6, 29.6, 29.7, 29.9, 29.9, 31.9 (−CH_2−), 69.2, 69.2, 69.4, 69.6, 73.6 (−CH_2−O−), 104.6 (═CH− pyrazole), 108.3, 111.3, 113.3, 113.6, 119.0 (Car-H), 141.5, 148.3, 151.0, 153.3, 153.3, 153.8, 153.8 (Car-O, Cpz). m/z (FAB$^+$) 1161 [M − Cl]$^+$.

Compound 3. Found: C, 70.9; H, 10.3; N: 1.9. Calcd for $C_{87}H_{152}ClN_2O_7Rh$: C, 70.8; H, 10.4; N, 1.9%. ν_{max}(KBr)/cm^{-1} 3153, 3120 (N−H), 2090, 2078, 2016 (CO), 1607, 1506 (arC−C), 1262 (C−O). δ_H (300 MHz; $CDCl_3$; Me_4Si) (see also Figure 2) 0.88 (m, 15H, CH_3−), 1.27−1.45 (m, 60H, −CH_2−), 1.45−1.55 (m, 10H, −CH_2−), 1.73−1.84 (m, 10H, −*CH_2*−CH_2−O−), 3.98−4.09 (m, 10H, −CH_2−O−), 6.59 (s, 1H, He), 6.71 (s, 0.8H, Hd), 6.9 (s, 1.2H, Hd′), 6.94−6.98 (m, J = 8.4 Hz, 1H, Hb, Hb′), 7.03 (d, J = 2.0 Hz, 0.6H, Hc′), 7.13 (dd, J = 8.4 Hz, J = 2 Hz, 0.6H, Ha′), 7.30 (m, 0.8H, Ha, Hc), 11.68 (s, 0.4H, Hf), 11.73 (s, 0.6H, Hf′). m/z (FAB$^+$) 1440 [M − Cl]$^+$.

Compound 4. Found: C, 68.4; H, 9.8; N, 2.1. Calcd for $C_{77}H_{132}ClN_2O_8Rh$: C, 68.4; H, 9.8; N, 2.1%. ν_{max}(KBr)/cm^{-1} 3405, 3300 (NH), 2078, 2009 (CO), 1601, 1584, 1488 (arC−C), 1240, 1115 (C−O). δ_H (300 MHz; $CDCl_3$; Me_4Si) 0.86−0.90 (m, 18H, CH_3−), 1.28−1.40 (m, 72H, −CH_2−), 1.34−1.51 (m, 12H, −CH_2−), 1.74−1.89 (m, 12H, −*CH_2*−CH_2−O−), 3.98−4.02 (m, 6H, −CH_2−O−), 4.07 (t, J = 6.4 Hz, 4H, −CH_2−O−), 4.24 (t, J = 7.2 Hz, 2H, −CH_2−O−), 6.65 (d, J = 2.4 Hz, 1H, He), 6.70 (d, J = 8.8 Hz, 1H, Hb), 6.95 (s, 2H, Hd), 7.28 (d, J = 8.8 Hz, 1H, Ha), 12.34 (d, J = 2.4 Hz, 1H, Hf). δ_C (75 MHz; $CDCl_3$; Me_4Si) 14.1 (CH_3−), 22.7, 26.0, 26.1, 29.3, 29.4, 29.4, 29.5, 29.6, 29.7, 29.8, 30.1, 30.3, 31.9 (−CH_2−), 68.9, 69.4, 73.6, 73.9, 75.0 (−CH_2−O−), 102.6 (═CH− pyrazole), 108.4, 108.5, 113.6 (Car-H), 122.5, 127.2 (Car-pz), 139.8, 141.8, 143.2, 150.9, 153.3, 155.0, 155.9 (Car-O, Cpz). m/z (FAB$^+$) 1317 [M − Cl]$^+$.

Compound 5. Found: C, 68.4; H, 9.8; N, 2.05. Calcd for $C_{77}H_{132}ClN_2O_8Rh$: C, 68.4; H, 9.8; N, 2.1%. ν_{max}(KBr)/cm^{-1} 3187, 3162, 3129 (N−H), 2084, 2078, 1997 (CO), 1592, 1504 (arC−C), 1245 (C−O). δ_H (300 MHz; $CDCl_3$; Me_4Si) 0.83−0.97 (m, 18H, CH_3−), 1.26−1.48 (m, 84H, −CH_2−), 1.71−1.87 (m, 12H, −*CH_2*−CH_2−O−), 3.99−4.08 (m, 12H, −CH_2−O−), 6.59 (s, 1H, He), 6.70 (s, 2H, Hd), 6.94 (s, 2H, Ha), 11.77 (s, 1H, Hf). δ_C (75 MHz; $CDCl_3$; Me_4Si) 14.1 (CH_3−), 22.7, 26.1, 29.4, 29.4, 29.6, 29.6, 29.7, 29.7, 30.3, 31.9, 31.9 (−CH_2−), 69.4, 73.6 (−CH_2−O−), 103.3 (═CH− pyrazole), 104.6, 108.2 (Car-H), 122.1, 126.7 (Car-pz), 139.9, 153.3, 153.8 (Car-O, Cpz). m/z (FAB$^+$) 1317 [M − Cl]$^+$.

Compound 6. Found: C, 46.5; H, 4.1; N, 4.7. Calcd for $C_{23}H_{24}ClN_2O_8Rh$: C, 46.4; H, 4.1; N, 4.7%. ν_{max}(KBr)/cm^{-1} 3186, 3153, 3129 (NH), 2093, 2084, 2011, 2001 (CO), 1591, 1572, 1503 (arC−C), 1244 (C−O). δ_H (300 MHz; $CDCl_3$; Me_4Si) 3.89 (m, 18H, CH_3O−), 6.61 (s, 1H, He), 6.77 (br s, 2H, Hd), 7.11 (br s, 2H, Ha), 12.18 (s, 1H, Hf). δ_C (75 MHz; $CDCl_3$; Me_4Si) 56.4 (CH_3O−), 61.0 (CH_3O−), 102.8 (═CH− pyrazole), 103.2 (br, Car-H), 106.2 (br, Car-H), 122.3 (br, Car-pz), 126.4 (br, Car-pz), 139.5 (Car-O), 153.4 (br, Car-O, Cpz). m/z (FAB$^+$) 559 [M − Cl]$^+$, 531 [M − Cl − CO]$^+$, 501 [M − Cl − 2CO]$^+$.

Crystal Structure Determination for L6 and 6·CH_2Cl_2. A summary of crystal data and refinement parameters is given in Table 1. Single-crystal X-ray diffraction data were collected on a Bruker SMART diffractometer equipped with an APEX CCD detector, with graphite-monochromated Mo Kα radiation (λ = 0.71073 Å), using the ω scan method. The crystals were covered with inert oil, mounted on glass fibers and cooled to the data collection temperature (100 K).

Table 1. Crystallographic Data for **L6** and **6**·CH_2Cl_2

	L6	**6**·CH_2Cl_2
crystal color, habit	colorless, irregular block	yellow, prismatic block
crystal size, mm^3	0.26 × 0.32 × 0.34	0.09 × 0.13 × 0.34
chem formula	$C_{21}H_{24}N_2O_6$	$C_{23}H_{24}ClN_2O_8Rh$·CH_2Cl_2
fw	400.42	679.73
cryst syst	tetragonal	monoclinic
space group	$I4_1/a$	$P2_1/n$
a (Å)	21.2193(16)	14.6971(14)
b (Å)	21.2193(16)	14.2494(14)
c (Å)	18.4841(14)	27.234(2)
β (deg)	90	94.254(3)
V (Å^3)	8322.6(11)	5687.8(9)
Z	16	8
D_{calcd} (g cm^{-3})	1.278	1.588
μ (mm^{-1})	0.094	0.930
θ range data collec (deg)	1.90-25.25	1.50-25.25
collected reflns	21937	33971
unique reflns	3768 (R_{int} = 0.0511)	10235 (R_{int} = 0.0756)
data/restraints/params	3768/0/298	10235/0/697
$R(F)$ [$F^2 > 2\sigma(F^2)$][a]	0.0396	0.0410
w$R(F^2)$ [all data][b]	0.0954	0.0824
S[c]	1.019	0.957

[a] $R(F) = \sum||F_o| - |F_c||/\sum|F_o|$, for 2899 and 7464 observed reflections, respectively. [b] w$R(F^2) = \{\sum[w(F_o^2 - F_c^2)^2]/\sum[w(F_o^2)^2]\}^{1/2}$. [c] $S = [\sum[w(F_o^2 - F_c^2)^2]/(n - p)]^{1/2}$; n = number of reflections, p = number of parameters.

Data were corrected for Lorentz and polarization effects and also for absorption using SADABS.[36] The organic structure (**L6**) was solved by direct methods using SIR97[37] and the rhodium complex by the Patterson method with SHELXS-97.[38] Both of these structures were completed with Fourier techniques and refined by full-matrix least squares on F^2 with SHELXL-97.[38] Atomic scattering factors, corrected for anomalous dispersion, were used as implemented in the refinement program. Anisotropic displacement parameters were used in the last cycles of refinement for all nonhydrogen atoms. Hydrogen atoms were placed in calculated positions, except those bonded to aromatic carbons and the nitrogen atom in compound **L6**, which were located in a difference Fourier map; all of them were refined riding on bonded atoms. Largest peak and hole in the final difference maps were 0.198 and −0.163 e Å^{-3} for **L6**, 0.944 and −0.620 e Å^{-3} for **6**·CH_2Cl_2. The program ORTEP-3,[39] in the WINGX package,[40] was used for diagrams.

Results and Discussion

Synthesis and Characterization of the Complexes in Solution. The rhodium complexes were readily obtained by reaction of the corresponding pyrazole ligands with [Rh(μ-Cl)$(CO)_2]_2$ in a 2:1 molar ratio. All complexes are air-stable materials and were isolated from the reaction media as yellow oils or pale-yellow waxy solids. Oils solidified upon storage in the refrigerator for several days. In solution these complexes are slightly unstable and decompose after several hours to give dark brown solutions. The analytical data and MS, IR, and NMR spectra are consistent with the proposed formulas.

The aromatic proton signals in the ^{1}H NMR spectra of samples in $CDCl_3$ are generally shifted upfield on complexation. Significant changes and the opposite trend are found for the NH signal. In the pyrazole ligands, the NH signal appears as an extremely broad signal at around 11 ppm due to fast interchange, and this signal is barely visible. A broad singlet in the region 11.5−12.3 ppm is clearly detected for the complexes. In all cases, resonances for the protons of the phenyl ring near the metal (Figure 2, Hd, Hg) are highly shielded and appear at lower chemical shifts than the corresponding protons near to the NH group (Figure 2, Ha, Hc).

Compound **6** displays two broad singlets for the resonances of the aromatic protons at room temperature, suggesting the existence of a metallotropic equilibrium (dynamic character resulting from site exchange of the metal between adjacent nitrogen atoms). However, the other complexes display sharp signals at room temperature, indicating that dynamic processes do not take place.

In particular, the long-chained compound **5** displays aromatic signals at slightly higher fields than the methoxy compound **6**, probably due to the shielding caused by folding of the decyloxy chains around the core.

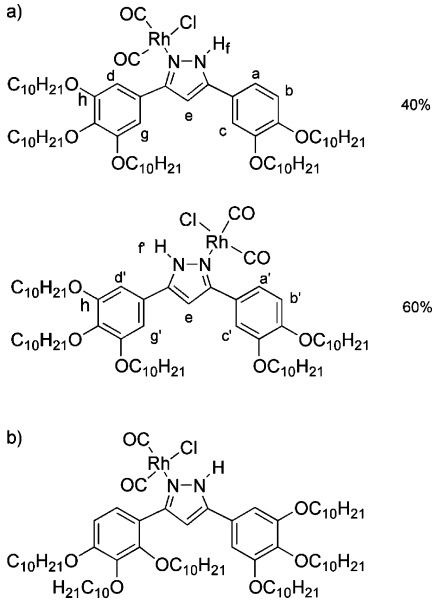

Figure 2. (a) Isomers found for **2**. The same proportion was found for **3** (with the same substitution in the phenyl rings but with C14 alkoxy chains). The ^{1}H NMR signals for the aromatic protons have been assigned in the Experimental Section according to these numbering schemes. (b) Structure of **4**.

Compounds **2** and **3** were obtained as mixtures of two isomers in a 3:2 ratio, as evidenced by the ^{1}H NMR spectra. This is a consequence of the nonsymmetrical substitution pattern of the ligand. Comparison of the spectra of the complexes, and also results of COSY and NOESY experiments, shows that in the major isomer the metal atom is situated next to the less-substituted aromatic ring (see Figure 2a). Two broad singlets for the NH proton can also be observed, and these are in the same ratio as found for the aromatic protons.

Compound **4**, although containing a nonsymmetrically substituted pyrazole, is formed as only one isomer. Therefore, metal complexation is influenced by steric effects imposed by the ligand. It appears that the rhodium atom only reacts with the less congested nitrogen atom, and in the case of compound **4**, this is next to the 2,3,4-tridecyloxyphenyl ring, assuming a conformation in which the decyloxy chain in the *ortho* position is far from the coordination site (Figure 2b). It can also be seen from the ^{1}H NMR spectrum an unusual ^4J coupling between the N−H and the C−H of the pyrazole, with both signals appearing as doublets with a coupling constant of 2.4 Hz. This is indicative of a slow proton interchange involving the NH in chloroform solution.

The IR spectra (KBr pellets) display sets of two, three, or four sharp bands in the 2090−1995 cm^{-1} region corresponding to the carbonyl stretching of mononuclear *cis*-dicarbonylrhodium(I) complexes. The pattern depends on the nature of the compound and also on the phase or state (see Experimental Section). Compound **6** was studied at different temperatures, and it was found that in the crystalline state at room temperature there are four bands for the carbonyl stretching vibration. These bands appear at 2093, 2084, 2011, and 2001 cm^{-1} and appear as two split absorptions of similar intensity. The splitting is attributed to solid-state effects as

(36) Sheldrick, G. M. *SADABS*, 2.03 ed.; University of Göttingen: Göttingen, Germany, 2002.
(37) Altomare, A.; Burla, M. C.; Camalli, M.; Cascarano, G. L.; Giacovazzo, C.; Guagliardi, A.; Moliterni, A. G. G.; Polidori, G.; Spagna, R. *J. Appl. Crystallogr.* **1999**, *32*, 115.
(38) Sheldrick, G. M. *SHELXS-97*, release 97-2; Institüt für Anorganische Chemie der Universität: Göttingen, Germany, 1998.
(39) Farrugia, L. J. *J. Appl. Crystallogr.* **1997**, *30*, 565.
(40) Farrugia, L. J. *J. Appl. Crystallogr.* **1999**, *32*, 837.

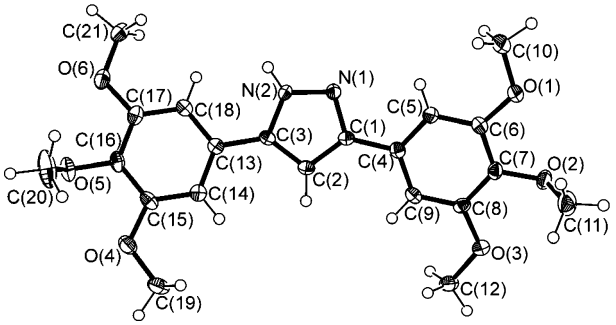

Figure 3. Molecular structure drawing for **L6**. ORTEP representation (50% probability ellipsoids) with atom numbering scheme. Selected bond distances (Å): N(1)−N(2) 1.354(2), N(1)−C(1) 1.342(2), N(2)−C(3) 1.354(2), C(1)−C(2) 1.397(2), C(2)−C(3) 1.382(2).

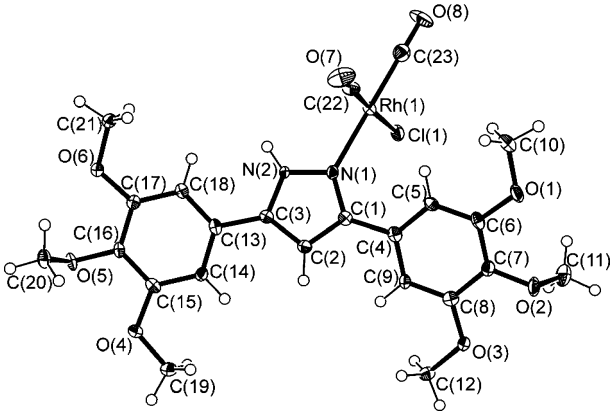

Figure 4. Molecular structure drawing for one of the two independent molecules of **6**. ORTEP representation (50% probability ellipsoids) with atom numbering scheme.

this phenomenon disappears at temperatures above the melting point. Indeed, in the isotropic liquid state (at 167 °C) there are two broad bands at 2080 and 2011 cm^{-1}. Weak N−H stretching bands are also found in the region 3200−3120 cm^{-1}, and these correspond to hydrogen bonded nitrogens. These bands are slightly shifted to higher wavenumbers on increasing the temperature, indicating a weakning of the hydrogen bonds in the isotropic liquid.

Single-Crystal Structure of Compound 6 and Its Pyrazole Ligand L6. Yellow prismatic single crystals of compound **6** were obtained by vapor diffusion of hexane into a solution of the compound in dichloromethane. **L6** was obtained as colorless plates from slow evaporation of a dichloromethane solution. Molecular drawings of these structures are shown in Figures 3 and 4. Selected bond distances for **L6** are included in Figure 3, and selected bond distances and angles for **6** are listed in Table 2.

In the crystal state, the pyrazole **L6** has a tetrameric structure supported by H-bonds, which form a 12-membered ring $(-N-N-H-)_4$. The internal symmetry of this tetramer is S_4 due to a crystallographic 4-fold inversion axis. Some other tetrameric structures, albeit with lower internal symmetry, have been described for 3,5-diphenylpyrazole[41,42] and

Table 2. Selected Bond Distances (Å) and Angles (deg) for **6**[a]

Rh(1)−Cl(1)	2.3687(10); 2.3621(10)	Rh(1)−N(1)	2.106(3); 2.099(3)
Rh(1)−C(22)	1.849(5); 1.853(5)	Rh(1)−C(23)	1.843(4); 1.845(4)
C(22)−O(7)	1.133(5); 1.134(5)	C(23)−O(8)	1.144(4); 1.143(5)
N(1)−N(2)	1.360(4); 1.347(4)	N(1)−C(1)	1.349(5); 1.356(4)
N(2)−C(3)	1.353(4); 1.356(4)		
Cl(1)−Rh(1)−N(1)	92.20(9); 88.72(8)	Cl(1)−Rh(1)−C(22)	175.47(13); 178.97(13)
Cl(1)−Rh(1)−C(23)	87.24(13); 92.06(13)	N(1)−Rh(1)−C(22)	89.32(14); 90.42(15)
N(1)−Rh(1)−C(23)	179.42(16); 179.10(15)	C(22)−Rh(1)−C(23)	91.25(18); 88.81(17)
Rh(1)−C(22)−O(7)	175.7(4); 178.5(4)	Rh(1)−C(23)−O(8)	179.7(4); 177.4(4)

[a] The two values correspond to the two independent molecules.

3-methyl-5-phenylpyrazole.[43,44] Each molecule interacts with both perpendicular molecules through two hydrogen bonds involving the acceptor and donor nitrogens of the pyrazole unit. In this way, two parallel molecules are situated perpendicular to the other two parallel molecules (Figure 5). In this compound, the steric hindrance introduced by the methoxy groups in positions 3 and 5 of the phenyl groups precludes the formation of planar dimeric structures as in, for instance, 3,5-diphenyl-4-bromopyrazole[41] or 3,5-bis(4-butoxyphenyl)pyrazole,[33] and the molecule adopts a globular organization that maintains the intermolecular H-bonding interactions. The supramolecular $(-N-N-H-)_4$ ring has a solvent accessible void or internal free volume of 53(3) $Å^3$ (calculated with the VOID[45] procedure as implemented in the PLATON[46] program). Stacking along the *c* axis gives rise to a channel-like supramolecular structure.

On the other hand, rhodium complex **6** crystallizes with two crystallographically independent molecules that have similar conformations. In this case, a parallel molecular dimeric structure is obtained, and in each molecule the coordination plane of the metal is rotated with respect to the pyrazole ring [66.50(11)° and 60.58(11)° for the two independent molecules]. The dimeric structure is formed through two weak H-bonds between the chloro atom of one molecule and the NH group of another one situated below (Figure 6). In the dimer, the Rh−Rh distance is 3.4456(5) Å. These parallel dimeric structures are arranged alternately in an antiparallel disposition and stacked along the *b* axis (Figure 7). The structure described here is rather unusual since in the previously studied $[RhCl(CO)_2(Hpz)]$ complexes the metal plane is coplanar to the pyrazole ring, showing NH···Cl intramolecular interactions, or almost coplanar (ca. 16°) to the pyrazole ring without H-bonding.[47−49] In compound **6**, the congested pyrazole structure and its tendency

(41) Aguilar-Parrilla, F.; Scherer, G.; Limbach, H.-H.; Foces-Foces, M. C.; Hernández Cano, F.; Smith, J. A. S.; Toiron, C.; Elguero, J. *J. Am. Chem. Soc.* **1992**, *114*, 9657−9659.

(42) Raptis, R. G.; Staples, R. J.; King, C.; Fackler, J. P., Jr. *Acta Crystallogr.* **1993**, *C49*, 1716.

(43) Maslen, E. N.; Cannon, J. R.; White, A. H.; Willis, A. C. *J. Chem. Soc., Perkin 2* **1974**, 1298.

(44) Moore, F. H.; White, A. H.; Willis, A. C. *J. Chem. Soc., Perkin 2* **1975**, 1068.

(45) van der Sluis, P.; Spek, A. L. *Acta Crystallogr.* **1990**, *A46*, 194−201.

(46) Spek, A. L. *J. Appl. Crystallogr.* **2003**, *36*, 7−13.

(47) Decker, M. J.; Fjeldsted, D. O. K.; Stobart, S. R.; Zaworotko, M. J. *Chem. Commun.* **1983**, 1525−1527.

(48) Torralba, M. C.; Cano, M.; Campo, J. A.; Heras, J. V.; Pinilla, E.; Torres, M. R. *J. Organomet. Chem.* **2001**, *633*, 91−104.

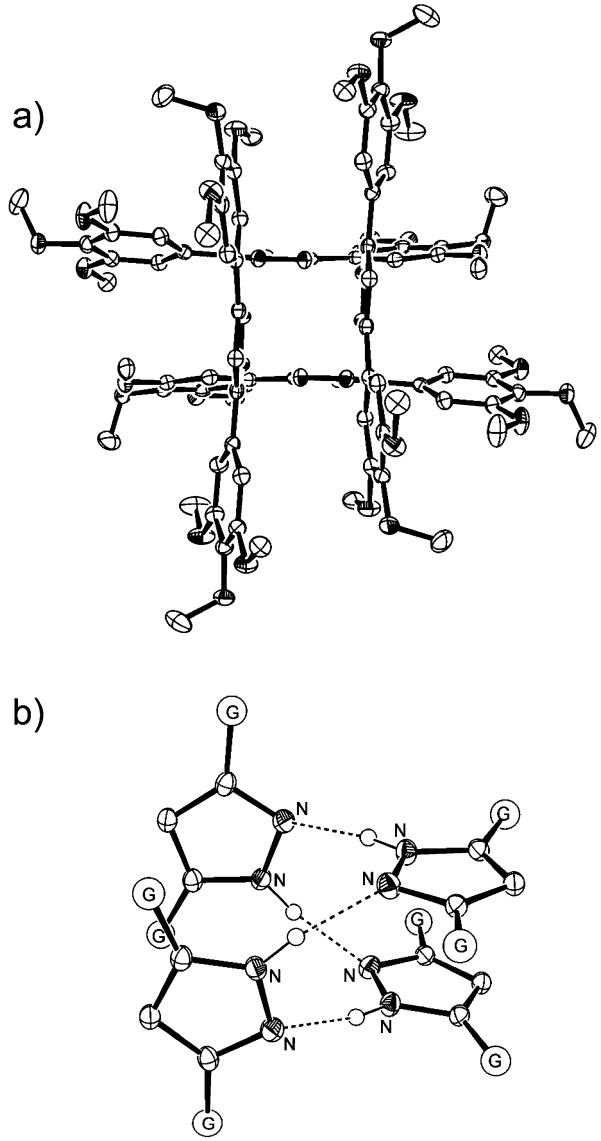

Figure 5. Tetrameric structure of ligand **L6**. (a) View along the *c* axis. (b) Detail of the intermolecular H-bonding pattern (G = 3,4,5-trimethoxyphenyl).

to stack may be responsible for the twisting of the metal plane in a staggered orientation with respect to the closest molecule to establish a double intermolecular NH···Cl bond. This tendency for stacking in **6** is more favorable than the structure exhibited by ligand **L6** in terms of forming a columnar mesophase.

Thermal and Mesomorphic Properties. Pyrazole ligands **L1**−**L6** are not liquid crystalline[27] although they could give rise to disk-shaped dimeric entities through hydrogen bonding, in a similar way to 3,5-bis(4-alkoxyphenyl)pyrazoles.[33]

DSC data corresponding to the first heating cycle for compounds **1**−**6** are gathered in Table 3.

It can be observed that the peripheral chain structure plays a crucial role in inducing mesomorphism. Compounds **1**−**4** are not liquid crystalline but are solids at room temperature, melting to the isotropic liquid with high enthalpies. The melting points decrease on increasing the number of aliphatic chains in the structure. Compound **1**, with four decyloxy chains, is a crystalline solid that melts directly to the isotropic liquid. An increase in the number of chains to five (compound **2**), elongation of the chain (compound **3**), or introduction of a six-chained ligand with reduced symmetry and steric hindrance (compound **4**) all gave rise to lower melting points and the absence of liquid crystal behavior.

It is interesting to note that compounds **2** and **4**, although they are not liquid crystalline, do not crystallize on cooling

(49) Cano, M.; Campo, J. A.; Heras, J. V.; Lafuente, J.; Rivas, C.; Pinilla, E. *Polyhedron* **1995**, *14*, 1139−1147.

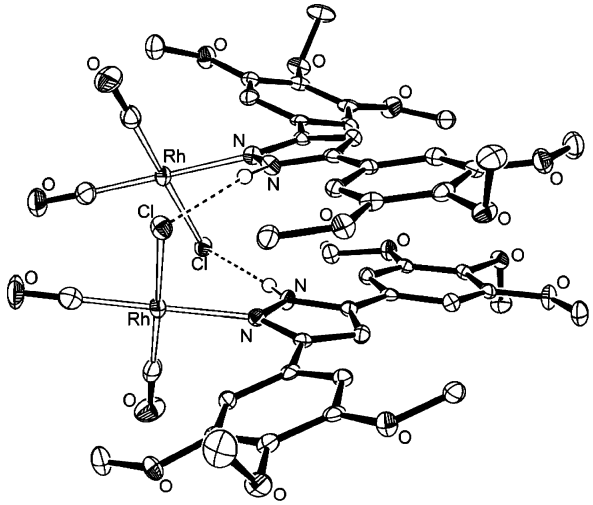

Figure 6. Dimeric structure of **6** held by double intermolecular H-bonds.

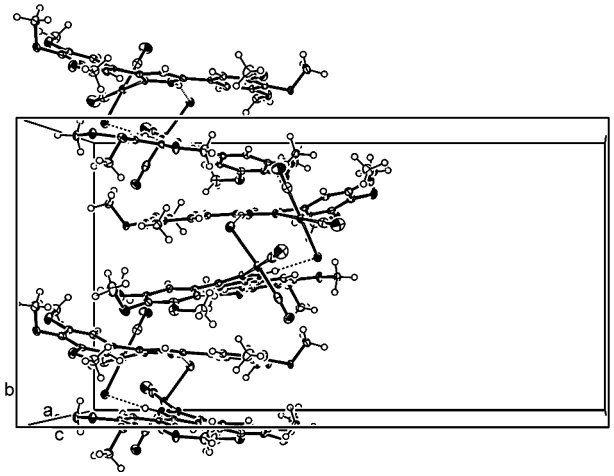

Figure 7. Packing of **6** along the *b* axis.

Table 3. Transition Temperatures and Thermodynamic Data for the DSC First Heating Cycle at 10 °C/min

compd	phase transition[a]	*T*, °C	Δ*H*, kJ mol^{-1}
1	Cr−I	91.3	72.23
2	Cr−Cr′	40.5	22.14
	Cr′−I	50.0	42.89
3	Cr−I	40.4	96.60
4	Cr−I	27.7	50.38
5	Cr−Col$_h$	31.4	45.96
	Col$_h$−I	46.9	2.08
	I−Col$_h$	45.7	−2.42
	Col$_h$−Cr	5.4	−48.75
6	Cr−I	147.9	22.42

[a] Cr, Cr′, crystal phase; I, isotropic liquid phase; Col$_h$, columnar mesophase.

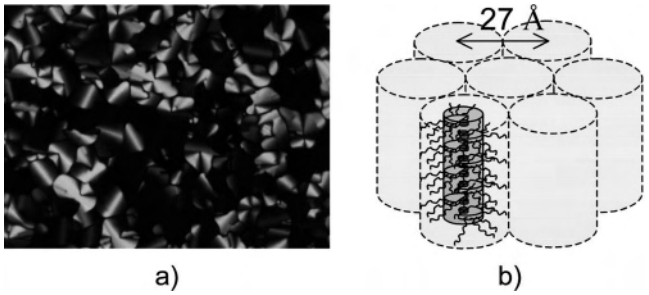

Figure 8. (a) Microphotograph of the texture of the columnar mesophase exhibited by compound **5** at 41 °C (crossed polarizers). (b) Proposed model for the columnar arrangement of **5**.

and remain as isotropic liquids at room temperature before becoming glasses at 14 and 0 °C, respectively. These glasses only crystallize over time on storing the samples in the refrigerator.

As one would expect, compound **6**, which does not contain long alkoxy chains, is not mesomorphic and has the highest melting point. On cooling, this material does not crystallize but becomes a glass at 80 °C and remains in this state over time.

Only complex **5** (with six decyloxy chains) is a liquid crystal. This compound shows an enantiotropic columnar mesophase in the range 31−47 °C before clearing to the isotropic liquid. On cooling, the mesophase reforms and remains down to 5 °C, when crystallization occurs. This mesophase shows a characteristic pseudo-focal-conic texture with large homeotropic areas (Figure 8a). The application of mechanical shear to the sample gives rise to a uniformly oriented birefringent texture.

In summary, induction of mesomorphism exclusively occurs in the case of compound **5**. The symmetrical pyrazole ligand with six decyloxy groups does not show mesogenic behavior, but the corresponding rhodium complex shows a columnar hexagonal mesophase that is stable at room temperature on cooling.

In an effort to determine the structure for the mesophase of **5**, this compound was studied by X-ray diffraction on an aligned sample obtained by mechanical stress at the mesophase temperature followed by freezing to room temperature.

The diffraction pattern is characteristic of a hexagonal columnar (Col_h) mesophase with a lattice constant $a = 27$ Å, as deduced form the d_{10} reflection (23.5 Å). As this reflection is located in the equator (plane perpendicular to the stress direction), the column axes are oriented parallel to the stress direction and the two-dimensional hexagonal lattice lies in the perpendicular plane.

In the large-angle region, an almost isotropic diffuse halo, characteristic of the disordered hydrocarbon chains, is observed at 4.6 Å. In addition, the diffraction pattern contains scattering bands perpendicular to the meridian corresponding to distances of 7.2 and 3.6 Å. The maximum at 3.6 Å corresponds to the stacking distance, and a combination of this value, the hexagonal lattice constant a, and the molecular mass (1352.24) allowed a density of 0.99 g cm^{-3} to be calculated, assuming that the mesophase of **5** consists of a hexagonal columnar assembly of molecules stacked 3.6 Å apart. The presence of scattering at 7.2 Å in the meridian region reveals the existence of an additional modulation of the electronic density along the column axis. A distance of 7.2 Å corresponds to twice 3.6 Å, and it can therefore be deduced that the molecular orientation alternates along the column axis in an antiparallel way. The value of 7.2 Å represents the distance between two equally oriented molecules.

High-temperature X-ray diffractograms recorded at 40 °C are very similar to those recorded at room temperature. Although oriented samples were not investigated, the patterns contained the same maxima as those described above. The difference is that the scattering maxima at 7.2 and 3.6 Å are weaker and more diffuse, which suggests a shorter correlation length of the stacking.

The structure proposed for **5** is promoted by the molecular shape, which resembles a half disk. Such molecules stacked in an alternating antiparallel way are able to generate columns with an almost circular cross section, consisting of an inner part containing the rhodium atoms and the aromatic rings and a peripheral part consisting of the disordered hydrocarbon chains uniformly spread around the inner core (Figure 8b). Indeed, in the antiparallel mode dipolar forces are satisfied. A similar type of organization with analogous lattice constants ($a = 27$ Å) has been found in the hexagonal columnar mesophases of some nondiscoid metal-containing and metal-free molecules with six decyloxy chains, which are joined together through interactions that involve the metal atom[7] or dipole−dipole forces.[50] The column diameter is smaller than twice the molecular radius, indicating that slight interdigitation exists between antiparallel neighbors.

In the columnar mesophase, it is very probable that NH···Cl interactions exist, as the IR N−H stretching frequencies of compound **5** in the mesophase are very similar to those found in the crystal of **6** (several bands between 3187 and 3129 cm^{-1}). However, it is not possible to clarify whether the H-bonding inside the columns is intermolecular or intramolecular in origin, as both would be consistent with the presence of stacked half-disks in an antiparallel arrangement in the mesophase. Therefore, the induction of mesomorphism in nondiscoid *cis*-[RhCl(CO)$_2$(Ln)] complexes is the result of a subtle combination of an appropriately substituted pyrazole, the planar arrangement of the pyrazole ligands in the complex, and the dipolar and/or hydrogen bonding interactions.

Spectroscopic Study of the Phase Transitions of Compound 5. Compound **5** exhibits marked changes in the phase transition from the crystalline state to the liquid crystal phase. This transition displays thermochromism that can be easily followed by the naked eye and is associated with changes in both the UV−vis (Figure 9) and IR (Figure 10) spectra.

Compound **5** in the crystalline state is a pale yellow solid and, at room temperature, shows a broad absorption band with a maximum at 277 nm and two shoulders at 305 and

(50) Omenat, A.; Barberá, J.; Serrano, J. L.; Houbrechts, S.; Persoons, A. *Adv. Mater.* **1999**, *11*, 1292−1295.

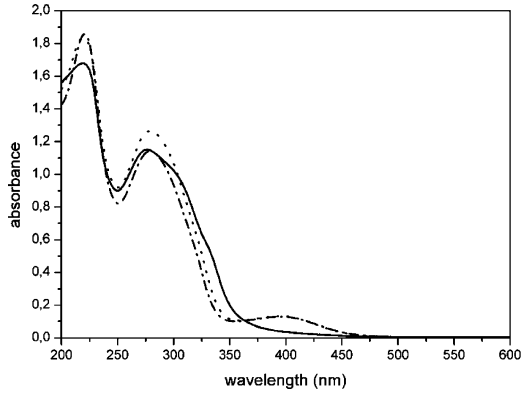

Figure 9. Variable temperature UV−vis spectra of **5**. Crystal phase at 25 °C (—). Columnar hexagonal mesophase at 42 °C (---). Isotropic liquid at 63 °C (— · —).

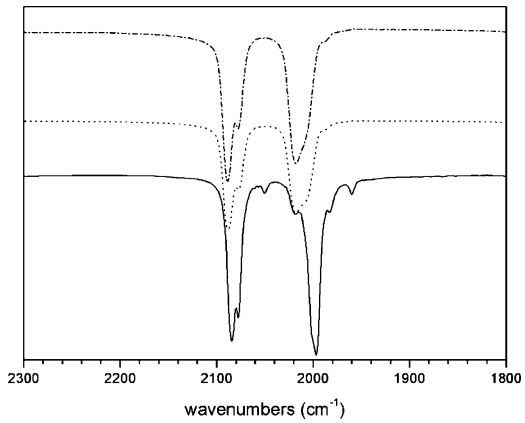

Figure 10. Variable temperature FTIR carbonyl stretching bands of **5**. Crystal phase at 25 °C (—). Columnar hexagonal mesophase at 42 °C (---). Isotropic liquid at 50 °C (— · —).

330 nm. When the compound enters the liquid crystalline phase, it changes to an intense yellow color, and in the UV−vis spectrum the highest energy band shifts slightly to 280 nm, the shoulders disappear, and a new band at 400 nm appears. The isotropic liquid shows the same spectrum as the liquid crystalline phase. Moreover, these latter two spectra are also similar to those observed in dilute solutions, although in solution the low energy band is much weaker compared with the rest of the bands.

On the other hand, the transition from crystal to liquid crystal is associated with a shift of the carbonyl stretching toward higher wavenumbers, indicating a decrease in the π-back-bonding in the metal−carbonyl bonds.

We can therefore assume that H-aggregates exist in the crystal, and on melting, they break and a new bathochromically shifted band appears at 400 nm that is related to the isolated molecule. This band at 400 nm can be assigned to a metal-to-ligand charge transfer (MLCT) band (d−π* character), which is also associated with stronger π-back-bonding of the metal−pyrazole bond and weaker π-back-bonding of the carbonyl−metal bond, as observed by IR spectroscopy.

It is worth mentioning that, in previously reported *cis*-[RhCl(CO)$_2$(HPz)] complexes, different sets and wavenumbers for the carbonyl stretching bands are found depending on the conformation of the pyrazole ligand with respect to the metal coordination plane and the intermolecular interactions in the crystalline state. Indeed, several different structures have been obtained for such complexes, and these include planar molecules with intramolecular NH−Cl bonds packed without metallic interactions, or unidimensional stacks of molecules with an out-of-plane angle for the pyrazole ligand of 16° and some degree of intermetallic interaction.[48] The low-frequency carbonyl stretching band for the former example appears at higher wavenumbers than for the latter. Therefore, the position of the carbonyl bands can be related not only to the degree of metal−carbonyl back-bonding and the metal valence but also to the conformation of the pyrazole ligand with respect to the metal coordination plane.

On the basis of a combination of the data found for these previously studied structures, the presence or absence of the intramolecular charge-transfer band, and the shifting of the carbonyl stretching band, we propose a more planar conformation in the mesophase than in the crystal state for compound **5**.

Conclusions

The induction of mesomorphism in nondiscoid *cis*-[RhCl(CO)$_2$(Hpz)] complexes **1**−**6** is the result of a combination of several factors. The most important is the ligand−ligand interaction, as only an appropriately substituted pyrazole with six decyloxy chains arranged symmetrically leads to liquid crystalline properties. Second, dipolar and hydrogen bonding interactions involving the chloro and the NH groups of a single molecule or neighboring stacked molecules are also important.

The columnar liquid crystal phase and the isotropic liquid are more similar to the isolated molecule, behaving as monomeric entities or systems with only weak intermolecular interactions. The spectroscopic data found in the mesophase are consistent with planar molecules exhibiting intramolecular NH−Cl bonds but packed without intermetallic interactions. This situation is also in agreement with the proposed structure from the X-ray experiments in the mesophase. However, aggregates exist in the crystalline state, and the low-energy intramolecular charge-transfer band disappears completely on cooling from the mesophase to the crystal, probably due to the pyrazole ligand being out of plane with respect to the metal coordination plane.

Acknowledgment. We thank the CICYT-FEDER MAT2003-07806-C02-01, BQU2000/1170, and the Programa Ramón y Cajal from the Ministerio de Educación y Ciencia (MEC), Spain, and the Gobierno de Aragón for financial support.

Supporting Information Available: Crystallographic data for **L6** and **6** as a CIF file. Figure S1 showing the molecular structure drawing for the two independent molecules of **6**. Figure S2 showing the XRD diffraction pattern of the mesophase of an aligned sample of compound **5**. This material is available free of charge via the Internet at http://pubs.acs.org.

IC0614216